Mapping growing stock volume and biomass carbon storage of larch plantations in Northeast China with L-band ALOS PALSAR backscatter mosaics

Tian Gao [a,b], J. J. Zhu [a,b,*], Q. L. Yan [a,b], S. Q. Deng [c], X. Zheng [a,b], J. X. Zhang [a,b], G. D. Shang [a,b,d]

[a] *CAS Key Laboratory of Forest Ecology and Management, Institute of Applied Ecology, Chinese Academy of Sciences, Shenyang, China*

[b] *Qingyuan Forest CERN, Chinese Academy of Sciences, Shenyang, China*

[c] *Institute of Mountain Science, Shinshu University, Nagano, Japan*

[d] *University of Chinese Academy of Sciences, Beijing, China*

* Correspondence author. E-Mail: jiaojunzhu@iae.ac.cn (J.J. Zhu); Tel.: +86-24-83970303; Fax: +86-24-83970300.

Mapping growing stock volume and biomass carbon storage of larch plantations in Northeast China with L-band ALOS PALSAR backscatter mosaics

Reliable spatial information on growing stock volume (GSV) and biomass is critical for creating management strategies for plantation forests. This study developed empirical models to map the GSV and biomass of larch plantations (LPs) in Northeast China (1.25 million km^2 total area) by integrating L-band synthetic aperture radar (SAR) data with ground-based survey data. The best correlation model was used to map the GSVs and biomasses of LPs. The total GSV and biomass carbon storage were estimated at 224.3 ± 59.0 million m^3 and 113.0 ± 29.7 10^{12} g C with average densities of 85.1 m^3 ha^{-1} and 42.9 10^6 g C ha^{-1}, respectively, over a total area of 2.64 million ha. The saturation effect of SAR was determined beyond 260 m^3 ha^{-1}, which was expected to influence the estimations for a small proportion of the study area. The accuracy of the estimations has limitations mainly due to the uncertainties in the GSV inventories, discrimination of natural larch and the SAR dataset. Based on the mapping results of the GSVs of LPs, a planning strategy for multipurpose management was tentatively proposed. This study can inform policies and management practices to assure broader and sustainable benefits from plantation forests in the future.

Keywords: larch plantation; growing stock volume; biomass carbon storage; Phased Array L-band synthetic aperture radar backscatter; saturation effects; Northeast China

Word Count: 8817

1. Introduction

Planted forests are an essential component of the terrestrial ecosystem and provide important ecosystem services to human society (Carle and Holmgren 2008). China possesses the largest area (69 million ha) of planted forests in the world, accounting for 26.1 % of the planted forest area in the world (Food and Agriculture Organization 2010; Chinese Ministry of Forestry 2014). According to the aims, the planted forests in China can be classified as protective forests for improving environmental conditions (e.g., harness soil and water losses) and productive forests for timber (Mason and Zhu 2014). The latter, which is traditionally defined as a "plantation forest", is normally afforested by a single species for convenient management (Kanninen 2010). Historically, plantation forests were partially developed from secondary forests. Since the 1950s, for example, primarily driven by the need for timber supply, larch (*Larix* spp.) has been widely planted in Northeast China as a commercial timber species with replacement of secondary forests (Zhu et al. 2010). Because larch is drought- and cold-resistant and grows rapidly, larch has become one of the most important timber species, playing an important role in meeting timber demands for the rapid economic development of China (Zhu et al. 2008). In recent years, however, several problems have been noticed in larch plantations (LPs), such as poor natural regeneration capabilities (Zhu et al. 2008; Yan, Zhu, and Gang 2013) and declines in soil fertility (Yang et al. 2010; Yang et al. 2012), which may have negative effects on the sustainability of ecosystem services. At the same time, facing the growing environmental threat and pressure from the promise to slash the CO_2

emissions of the country, "ecological civilization" that aims to improve the environment has been presented as the national strategy of China since 2013, and forestry occupies a crucial role in this strategy framework (UNDP and IUES 2013). There is a growing demand for plantation forests to be proposed for environmental and conservation aims. The historical plans and management practices (e.g., logging regime) for plantation forests may no longer be able to adapt to the needs of policymakers due to shifted purposes. Accurate, detailed, and up-to-date spatial and structural information on a plantation forest is essential for understanding its services and further designing optimum forest management strategies and policies.

Growing stock volume (GSV) is defined as the stem volume of all living trees in a stand and is a fundamental indicator for plantation forests since it represents the commercial timber wood volume of a stand. Traditionally, the methods used to estimate the GSV of a forest over broad geographical scales rely on field-based surveys. First, the diameter at breast height (DBH) for each tree is measured, which is used to calculate the stem volume. Then, the volumes of all trees within a sampling site are summed to estimate the GSV of a stand. Finally, the surveys at the site level are extrapolated at provincial or national levels. Nevertheless, there are two problems that hinder the availabilities of field-based methods. Since GSVs are typically estimated from limited field samples, the extrapolated GSV estimates have high uncertainties (Saatchi and Moghaddam 2000). In addition, field-based surveys do not include the explicit distribution of the GSV of a forest, which is crucial for plantation forest management practices (e.g., logging). A wall-to-wall estimate that combines satellite-based imagery with field-based forest measurements can help address these issues (Immitzer et al. 2016). By integrating remote sensing image with field-based GSV data, the relationship between raster values and ground GSV measurements can be established, and a spatially continuous GSV can be mapped; thus, this method has been widely used to estimate the GSV of a forest over large spatial scales (Santoro, Eriksson, and Fransson 2015; Schlund et al. 2015).

Compared to optical remote sensing, synthetic aperture radar (SAR) is a powerful tool that can be used to retrieve information on forest structure due to its sensitivity to geometric attributes (Karam et al. 1995). Previous studies have presented a positive logarithmic relationship between SAR backscatter and GSV (Avtar, Suzuki, and Sawada 2014; Chowdhury, Thiel, and Schmullius 2014; Hamdan, Khali Aziz, and Mohd Hasmadi 2014; Santoro, Eriksson, and Fransson 2015; Thiel and Schmullius 2016), and the general experiences indicate that SAR data at long wavelengths (L-band) are more appropriate for GSV estimations than data at shorter wavelengths (X- and C-bands) (Rosenqvist et al. 2007; Peregon and Yamagata 2013). The adequacy of L-band SAR data has been reported for tropical forests (Cutler et al. 2012; Rahman and Tetuko Sri Sumantyo 2012), savanna woodlands (Mitchard et al. 2009; Mermoz et al. 2014), mangroves (Hamdan, Khali Aziz, and Mohd Hasmadi 2014), temperate forest (Cartus, Santoro, and Kellndorfer 2012; Robinson et al. 2013), boreal forests (Pantze, Santoro, and Fransson 2014; Wilhelm et al. 2014) and plantations (cashew and oil palm) (Morel, Fisher, and Malhi 2012; Avtar, Takeuchi, and Sawada 2013). Nonetheless, wall-to-wall estimates of the GSV of plantation forests at a regional scale have not been reported. On the other hand, the availability of L-band SAR data for GSV estimation primarily struggles with the problem linked to the saturation effect (the sensitivity of SAR backscatter decreases with increases in GSV). While saturation levels have been examined for multiple forest types, these studies were carried out at regional scales that involved various forest types. Saturation effects are site dependent and are closely linked to forest structures and environments (e.g., moisture conditions) (Lucas et al. 2010). Various forest structures and environmental conditions at a regional scale may cover up the difference in saturation levels among forest types (i.e., natural forests and plantation forests). As the area of plantation forests is rapidly increasing worldwide, the contributions of plantation forests are expected to become increasingly important (Kanninen 2010). However, the saturation effect of L-band SAR for monitoring plantation forests is not well documented, and the potential of using L-band SAR for the estimation of the GSV of plantation forests remains unclear.

As a key component of the terrestrial ecosystem, the biomass of a forest determines its ecosystem services, such as timber production, prevention of soil loss by wind and runoff, and carbon sink (Costanza et al. 1997; Pan et al. 2011). Quantitative information on the carbon stocks of forest biomass is critical for forest ecosystem service assessments. Volume-derived biomass estimation is an appropriate method that has been widely used to estimate forest biomass at large scales (Brown and Lugo 1984; Turner et al. 1995). The volume-derived biomass method was originally designed to use stem data to obtain reliable biomass or carbon stock estimates because most forest inventories record information regarding sellable timber volume (Sharp, Lieth, and Whigham 1975; Fang et al. 1998). For the volume-derived biomass methodology, the key parameter is the ratio of total stand biomass to stem volume (Fang and Wang 2001). Previous studies reported that the ratio varied with forest type, site condition, age-class and management practice (Schroeder et al. 1997; Brown, Schroeder, and Kern 1999; Fang et al. 2001). Accordingly, Fang et al. (2001) improved a method to calculate the contentious ratio of total stand biomass to stem volume, and this method has been used to estimate biomass carbon storage at national and global levels (Pan et al. 2011). Previous studies based on the volume-derived biomass method have mostly focused on the "size of forest biomass carbon stock" (amount), which is considered a key component of carbon budget assessments (Fang et al. 2001; Pan et al. 2011). Although biomass quantifications can be obtained at the province, forest type and age-class levels (Guo et al. 2013), the explicit spatial distribution of forest biomass is still lacking. For plantation forests especially, the pattern is valued for informing forest management policies.

This study sought to evaluate the performances of multiple ALOS PALSAR (Advanced Land-Observing Satellite Phased Array L-band Synthetic Aperture Radar) backscatter-derived variables for mapping the GSV of LPs in Northeast China by using field survey samples and an ALOS PALSAR dataset. The study also improved upon the volume-derived method to obtain the continuous spatial distribution of LP biomass. By assessing the GSV and biomass carbon storage estimates from LPs, this study provides insights into the prospects of LPs.

2. Data and Methods

2.1 Study area

This study was conducted in the northeast part of China, which is defined here to include Liaoning Province, Jilin Province, Heilongjiang Province, eastern Inner Mongolia Autonomous Region and northern Hebei Province (115 °E – 135 °E, 38 °N – 53 °N; about 1,250,000 km^2). As shown in Figure 1, the study area is characterized by plains separated by five major mountain ranges, with a west-east distribution of the Yanshan Mountains, Daxing'an Mountains, Xiaoxing'an Mountains, Zhangguangcai Mountains and Changbai Mountains. These mountains are the sources of the main rivers in Northeast China, including the Songhua River, the Liao River and the Yalu River. The climate in Northeast China is controlled by the East Asia monsoon, showing warm temperate, temperate and cool temperate zones from south to north, and humid, semi-humid and semiarid zones from east to west (Wang et al. 2008). Northeast China is one of the most important forest regions in China. Since the 1950s, LPs have been planted on approximate 2.6 million ha in Northeast China, accounting for 84.2 % of the total LP area of the country.

2.2 Field data

The LP volume data and interpretation locations were collected over large geographic extents across Northeast China between July and October of 2013 to 2015. The sampling sites, as well as the LP interpretation locations, covered the main distribution of LPs, including the Yanshan Mountains, Daxing'an Mountains, Zhangguangcai Mountains and Changbai Mountains (Figure 1). Each plot was established at least 15 m from the border of a LP patch for its representative, and each plot had a dimension of 30 m × 30 m. Trees with DBH values less than 6 cm were defined as saplings, and the stem volumes of saplings are too small to be considered in the GSV estimation. In addition, most of the stem volume equations are available for trees with DBH values greater than 4 cm; thus, the stems of trees with DBH values ≥ 4 cm were measured in each plot (Meng et al., 2006). In addition, tree density and age were recorded. To calculate the stem volume accurately, local stem volume equations were employed to estimate the stem volumes of the sampled trees in a given area (Table 1).

The stem volume of all trees in a sampling plot were summed as the GSV of the plot, and 316 field samples were obtained. In addition to the above sample data, another 64 plots were compiled from the Forest Resource Management Inventory (FRMI) from 2011 to supplement our field surveys. The FRMI is usually conducted by local forestry administrations, aiming to support forest management and planning. Following representative principles, the FRMI survey method is similar to the survey in this study, including the DBH measurements and the same stem volume equations for volume calculation. However, the FRMI sampling plot is not the same size of 30 m × 30 m for a LP patch, and rectangular and circular plot shapes were also employed in the FRMI. Since LPs were planted and managed (e.g., thinning) as patches, the trees within a patch are relatively homogeneous; thus, the effects of different sampling methods on the survey results were limited. To temporally match the SAR data (2010), the empirical annual increments of GSV that linked multiple LP ages (Gu

1987; Saihanba Forestry Center 2012), as well as the thinning records that were provided by the local forestry administration, were employed to adjust the GSVs of the LPs to those of 2010. Finally, a total of 380 samples with units of m^3 ha^{-1} were obtained to train and test the GSV estimation models.

2.3 SAR data and processing

PALSAR data were acquired from Northeast China by the ALOS mission of the Japanese Aerospace Exploration Agency (JAXA), which was launched in January 2006 and operated until April 2011. The ALOS PALSAR mosaic at HH (horizontal transmit and horizontal receive) and HV (horizontal transmit and vertical receive) polarizations have been open to the public for free downloads since 2014 (Shimada et al. 2014). To generate the ALOS PALSAR mosaics, the HH and HV data that were acquired between June and October were used, and the original strip data that show minimum responses to surface moisture were preferentially selected to produce the PALSAR mosaic (Shimada et al. 2014).

All supplied mosaics were already geometrically corrected and radiometrically calibrated, as well as adjusted for seasonal changes between adjacent strips. In this study, ALOS PALSAR HH and HV data from 2010 were used in 1 ° × 1 ° mosaic tiles (about 111 km × 111 km) with a pixel spacing of 25 m × 25 m. A median filter of 5 pixel × 5 pixel was employed to reduce speckle effects (Lee et al. 2009). The digital number (DN) signal was converted into gamma-naught (γ^0) using the following equation (Shimada et al. 2010):

$$\gamma^0 = 10 \cdot \log_{10}(\mathrm{DN})^2 - 83 \tag{1}$$

where DN represents 16 bits unsigned integer digital numbers.

Previous studies have reported that the transformation of the original HH and HV bands may improve the saturation point for biomass or GSV estimations (Mougin et al. 1999; Sarker et al. 2012; Hamdan, Khali Aziz, and Mohd Hasmadi 2014). For example, Hamdan, Khali Aziz, and Mohd Hasmadi (2014) found that patches of matured mangrove stands appeared brighter than stands that were newly planted when the images were produced by manipulating the polarizations, such as HH / HV and $(HH \cdot HV)^{-1/2}$. To examine this potential for the estimations of the GSV of LPs, the PALSAR backscatter-derived variables were calculated, including HV / HH, $(HH + HV) / 2$ and $(HH \cdot HV)^{-1/2}$.

2.4 Mapping larch plantation

Understanding the distribution of LPs is a prerequisite for investigations on the GSV and biomass of LPs. Larch is a coniferous and deciduous tree species that can be identified by its remarkable seasonal changes (Gao et al. 2015). During the growing season, larch can be discriminated from a broadleaf forest by the spectra of its coniferous features; during the non-growing season, larch drops its leaves, which allows it to be discriminated from the other evergreen coniferous tree species. To identify the unique phenological behaviors of larch, a Landsat dataset with a spatial resolution of 30 m was applied, which was captured during the growing season (leaf on, between June and October) and non-growing season (leaf off, between November and March) of 2010. In cases where the data availability was limited (e.g., cloud-covered images), images were selected from the following year. The cloud coverage of each of image was less than 10.0 %, and the images where clouds did not cover the LP area were preferred. A total of 164 cloudless scenes were finally collected, consisting of 82 scenes for each season. These scenes were collected from the United States Geological Survey (USGS) and had been processed to the L1T level (orthorectified). Geometric correction was performed to reduce the error to less than 15 m. Then, the Landsat images were converted into reflectance values using the radiative transfer "code" based on MODTRAN4 (Rodriguez-Galiano et al. 2012), which was performed using the Fast Line-of Sight Atmospheric Analysis of Spectral Hypercubes (FLAASH) software package in ENVI 5.0.

False color composites were selected for the Landsat images with green (530 – 590 nm), red (640 – 670 nm) and near-infrared (NIR) bands (850 – 880 nm) to enhance the separability between forest types. At the pixel level, unsupervised classification (*k*-means) was employed for the summer images to discriminate coniferous forests by visually identifying the coniferous forests. Then, the same method was applied to the winter images to extract the evergreen coniferous forests. The number of classes was set up within the range of 20 to 25, and the maximum iterations were 10 to 15. The classification results were visually inspected, and the classification procedure was repeated after changing the *k*-means parameters, depending on the classification results.

The spatial distribution of larch was finally obtained by overlaying the two results. The discrimination of natural larch is a practical problem. Natural larch is mainly distributed through some areas in Jilin Province, Heilongjiang Province, and eastern Inner Mongolia Autonomous Region, whereas there is no natural larch in Liaoning Province or northern Hebei Province. The National Forest Resource Inventory data for China (2009 to 2013) were used to exclude natural larches from the interpreted results (Chinese Ministry of Forestry 2014). In addition, LPs in Northeast China are mostly single species monocultures and were originally planted as patches. A visual inspection was employed to distinguish the texture features and shapes to exclude natural larch. The final LP mapping results were tested by field-based interpretation, and an accuracy of 92.5 % was obtained. LP mapping is time-consuming work, and more detailed descriptions of LP mapping can be found in the study from our research group reported by Shang et al. (2017).

2.5 Estimation of GSV

Since the GSV or biomass of a forest is logarithmically correlated to SAR backscatter (Sandberg et al. 2011; Hamdan, Khali Aziz, and Mohd Hasmadi 2014), logarithmic regression models were employed in this study for the GSV estimations. The LP GSVs were estimated by the following three steps. First, the field-based GSVs were correlated to the spatially corresponding pixel backscatter of the PALSAR polarizations, as well as the three variables transformed by the original HH and HV polarizations, and a database was established. Second, the database was applied to train logarithmic regression models by randomly selecting 70.0 % of the total records (Figure 2). Third, the root mean squared error (RMSE) values were calculated with the reserved records to evaluate the performances of these models for GSV estimation.

$$\mathrm{RMSE} = \sqrt{\frac{1}{N}\sum_{i=1}^{N}\left(Y_{\mathrm{P},i} - Y_{\mathrm{O},i}\right)^2} \quad (2)$$

$Y_{\mathrm{P},i}$ and $Y_{\mathrm{O},i}$ represent the retrieved-GSV and ground-truth GSV, respectively, and N is the sample number.

2.6 Estimation of biomass carbon storage

The volume-derived biomass method was used to estimate the LP biomass in Northeast China. Here, the biomass expansion factor (BEF) is defined as the ratio of total stand biomass to GSV and can be expressed as a reciprocal equation (Fang and Wang 2001):

$$\mathrm{BEF} = a + b / x \quad (3)$$

where x (m^3 ha^{-1}) is the stand stem volume per unit area (GSV); a and b are constants for a specific forest type, which were assigned as 0.610 and 33.806, respectively, in this study (Guo et al. 2010). Spatially continuous BEF values that were based on the GSV distribution were mapped (Section 2.5). Then, the BEF combined with GSV data were used to map the LP biomass (t ha^{-1}) for the entire study area. Finally, the biomass carbon storage was obtained by converting the biomass into units of carbon (t ha^{-1}) with a coefficient of 0.5.

2.7 Definitions of saturation level

A limitation of SAR is that saturation effects occur at higher GSV levels, leading to the loss of predictive power for GSV (Imhoff 1995; Peregon and Yamagata 2013), and defining the saturation level is indispensable for understanding the applicability of the estimation. To quantify the uncertainty caused by the saturation effect, two saturation level definitions were employed: the fitted asymptote between GSV or above ground-biomass (AGB) and backscatter increases less than 0.01 dB, corresponding to an increase in AGB of 10^6 g ha^{-1} (Lucas et al. 2010), and the asymptote increases less than 0.20 dB, corresponding to an increase in AGB of 10^6 g ha^{-1} (Mermoz et al. 2014). The root: shoot biomass ratios of 0.2 were used to obtain the AGB and estimate the saturation level (Wang, Fang, and Zhu 2008).

3. Results

3.1 ALOS PALSAR backscatter-based variables versus GSV for LPs

The five ALOS PALSAR backscatter-based variables were related to ground GSV to develop logarithmic regression models (Figure 2). The highest model accuracy was established by the (HV + HH) / 2 variable, following by HV, $(HH \cdot HV)^{-1/2}$, and HH. The HV / HH variable did not show a significant relationship with GSV. Therefore, the (HV + HH) / 2 variable was selected for the GSV prediction model.

The (HV + HH) / 2 backscatter of all corresponding sampling plots ranged from – 6.39 dB to – 19.79 dB, with a mean of – 9.33 dB. The backscatter increased asymptotically with GSV. The changes in backscatter per increase in GSV of 10 m^3 ha^{-1} were 0.25 dB, 0.16 dB, 0.12 dB, and 0.10 dB at GSV levels of 100 m^3 ha^{-1}, 150 m^3 ha^{-1}, 200 m^3 ha^{-1} and 250 m^3 ha^{-1}, respectively, showing a decrease in sensitivity. According to the two saturation level definitions (Section 2.7), the saturation levels of the variable (average of HH and HV) for the retrieval of the LP GSV are 260 m^3 ha^{-1} (backscatter less than 0.20 dB per 10^6 g ha^{-1}) and 490 m^3 ha^{-1} (backscatter less than

0.01 dB per 10^6 g ha^{-1}), respectively. The model validation supported the lower saturation level definition, indicating that the sensitivity of the predictive variable decreased at a GSV of 250 m^3 ha^{-1} (Figure 2 (*f*)). If the lower saturation level (260 m^3 ha^{-1}) was taken into consideration, only a small proportion (< 0.2 %) of the area was affected, suggesting that the saturation effect weakly influenced the retrieval of LP GSV. If the test samples with GSV values greater than 245 m^3 ha^{-1} were not included in the model validation, the RMSE and relative RMSE (rRMSE, i.e., the RMSE divided by the averaged GSV) would reach ± 33.1 m^3 ha^{-1} and 26.3 %, respectively (Table 2).

3.2 Mapping GSV and biomass carbon storage of LPs

The optimum regression model that was fitted by the average of HV and HH was applied to map LP GSV at a pixel level with 25 m spatial resolution (Figure 3). The total LP GSV over Northeast China (LP area of 2.64 million ha) was estimated to be 224.3 million m^3, with an average GSV density of 85.1 m^3 ha^{-1}.

Spatially, LP GSV shows substantial heterogeneity without an obvious trend. Low GSV density (< 40 m^3 ha^{-1}) was observed in the southern part of the Inner Mongolia Autonomous Region near the forest-steppe ecotone between the Daxing'an Mountains and Horqin Steppe and in northern and eastern parts of Heilongjiang Province. A medium-low GSV (40 to 75 m^3 ha^{-1}) was observed in the mid-eastern part of Jilin Province and northern part of the Inner Mongolia Autonomous Region, as well as the northern and eastern parts of Heilongjiang Province. Medium-high GSV (75 to 145 m^3 ha^{-1}) appeared in the eastern part of Liaoning Province, northern part of

Hebei Province, eastern part of the Inner Mongolia Autonomous Region and middle part of Heilongjiang Province. High-density GSV (> 145 m^3 ha^{-1}) appeared in the mid-eastern part of Liaoning Province and a small area in the middle part of Heilongjiang Province.

The BEF mainly ranged from 0.8 to 1.4, with a mean of 1.1. Based on the estimated GSV and BEF, the biomass carbon storage (above- and belowground biomass) of LPs was assessed to be 113.0 10^{12} g C, with a mean biomass density of 42.9 10^6 g C ha^{-1} (Figure 4). The spatial biomass carbon storage pattern was consistent with the GSV distribution.

4. Discussions

4.1 Saturation effect for the estimation of GSV

The saturation level of the ALOS PALSAR variable (average of HH and HV) was 260 m^3 ha^{-1} in this study, suggesting that the saturation effect is weak for the estimation of LP GSV. The saturation effect is site dependent and is influenced by the different observed objects as well as the various environmental conditions (Sandberg et al. 2011). Since saturation levels can be represented by aboveground biomass or GSV, these results were unified by an expression of aboveground biomass to compare saturation levels among different studies (Table 3). Saturation levels have been examined to occur in wide AGB values ranging from 100 to 200 10^6 g ha^{-1}. The saturation levels for temperate and boreal forests were observed to exceed 140 10^6 g ha^{-1} (Cartus, Santoro, and Kellndorfer 2012; Chowdhury, Thiel, and Schmullius 2014;

Thiel and Schmullius 2016). The saturation levels for cashew plantations (Avtar, Suzuki, and Sawada 2014), mangroves (Hamdan, Khali Aziz, and Mohd Hasmadi 2014), tropical forests (Saatchi et al. 2011), and savannas (Mermoz et al. 2014) were lower than those of temperate and boreal forests. Our observed saturation level is higher than that observed in most previous studies, and this finding can be interpreted as follows. Most of the LPs in China are afforested as a single species monoculture and an even-aged structure, and the undergrowth vegetation is sparse. This simple stand structure can enhance the proportion of backscatter from the tree stem (Watanabe et al. 2006). Furthermore, the large area of this study also contributes to the high saturation levels. The wide ranges of GSV and the corresponding ALOS PALSAR backscatter resulted in the steep slope of the regression fit the logarithmic curve (Lucas et al. 2010). These results suggested that the ALOS PALSAR data were well adapted to monitor plantation forests and estimate their biophysical parameters at a large spatial scale.

4.2 Uncertainty assessment

Taking the rRMSE of 26.3 % into consideration, the total LP GSV can be estimated to range between 165.3 and 283.3 million m^3 in Northeast China. Since the estimated biomass value was linearly related to the estimated GSV, the modeling error can be directly applied to the biomass, which can be estimated to range from 83.2 to 142.7 10^{12} g C. In addition to the modeling error, the estimation accuracy for this large geographic extent still contains some limitations due to the uncertainties in LP mapping, sampling errors, GSV calculations and SAR data. Although extensive work has been conducted to improve the discrimination accuracy for LPs (Section 2.4), the estimation results still contained errors, such as the discrimination of natural larch. Since the GSV of natural larch may be greater than that of a LP, this misclassification would result in the overestimation of GSV, which mainly occurred in the Daxing'an Mountains. In addition, since larch was planted as patches and the management practices (e.g., thinning) were also conducted in the patches, the area within the same patch is generally homogenous. In the LP mapping process, the misclassified and mixed pixels mainly appeared in the marginal areas, leading to the increased uncertainty in the GSV estimations.

Another possible uncertainty is from sampling errors. The sampling errors are related to the limited sizes and locations of the study plots, which may not represent the general level of a sampled LP patch (Chave et al. 2004). In addition, the two field survey datasets that were produced by our sampling team and the FRMI were combined to train and validate the GSV estimation models. Although the two datasets were generated with similar sampling principles and measures, there were differences in the sampling practices. Considering the homogeneity of a plantation forest patch, the uncertainty induced by sampling errors can be expected to be small.

The GSV calculation of sampling sites also produces errors. Here, only LPs were considered, and site-specific allometric models were chosen for the stem volume calculations; thus, we imply that this error would be less than 5.0 % (Chave et al. 2005; Mermoz et al. 2014). Furthermore, the empirical annual increases in GSV were employed to temporally match the field survey samples with remote sensing data.

412 Since various site conditions of LPs cannot be taken into consideration in the annual GSV increases, the age-related empirical values were used. This simplification would homogenize the annual increases in the GSV of LPs with different site conditions for 3 to 5 years.

416 Finally, the largest uncertainty for the LP GSV estimation would be induced from the SAR datasets with large geographic extents and terrain effects, including the radiometric accuracy, speckle noise, and geometric accuracy of the dataset. The ALOS PALSAR mosaic data used in this study were preprocessed by selecting through visual inspection to minimize the surface moisture response. This seasonal change (wet and dry season) of the backscatter coefficient was limited to less than 0.20 dB in both HH and HV polarizations (Shimada et al. 2014). If the LPs with average backscatters of –9.33 dB were considered as reference objects, the seasonal variation in the backscattering coefficient leads to a GSV estimation error of approximately ± 5.4 m^3 ha^{-1}, accounting 16.3 % of the GSV estimation RMSE. In addition, ALOS PALSAR mosaic data were produced by 16 looks (Shimada et al. 2014), and a median filter of 5 pixel × 5 pixel was employed to reduce the speckle achieved in this study (Section 2.3). To reduce the terrain effects on the backscattering coefficient, the ALOS PALSAR images were orthorectified and slope-corrected using a 90 m Shuttle Radar Topography Mission Digital Elevation Model (Shimada et al. 2010). This process obtained a geometric accuracy of 12 m for the ALOS PALSAR mosaic, assuring close correspondence between the sampling sites and image pixels. Although these efforts were made to correct the PALSAR

data, the radiometric and geometric errors caused by incomplete calibration remained; for example, there were seasonal differences between strips due to soil moisture (Shimada et al. 2009). This uncertainty has been considered a challenge to improving the accuracy of forest GSV or biomass estimations through satellite-based SAR data (Slayback, Pinzon, and Tucker 2003; Shimada and Ohtaki 2010).

4.3 Implications of the GSV and biomass estimates for LP management

The LP GSV in Northeast China was estimated to be 224.3 million m^3, with a mean density of 85.1 m^3 ha^{-1}. As a dominant timber species that has been afforested in North China since the 1960s, this GSV is low for meeting the timber demands of China. As reported by the Chinese Ministry of Forestry (2015), the timber demands of China are 539 million m^3. This result means that even if all LPs in Northeast China were harvested, they could provide less than half of the timber demands of China for one year. During the past two decades, the plantation forest patterns have undergone profound changes. On the one hand, the fast-growing plantation forests of South China developed rapidly. For example, although the eucalyptus plantation area accounts for merely 2.2 % (4.5 million ha) of the forest area of China, eucalyptus contributed to 26.9 % (> 30 million m^3) of the timber production of China (Peng 2015). In addition, the bamboo forests of China increased from 3.2 million ha in the 1980s to 6.0 million ha in the 2010s (Chinese Ministry of Forestry 2014). These fast-growing plantation forests provide a large number of wood goods, including roundwood and fiber, which partly substituted the timber supply from traditional plantation forests in North China. On the other hand, the wood-based panel (plywood, medium density fiberboard, particleboard, etc.) industry of China has experienced dramatic development. Wood-based panel production increased by approximately one hundred times from 2.0 million m^3 in the early 1990s to 274 million m^3 in 2014, accounting for 60.0 % of the wood-based panel production in the world (Chinese Ministry of Forestry 2015). Consequently, the developments of fast-growing forest plantations and the wood-based panel industry mitigate the pressure on timer production that is supposed to be produced by traditional plantation forests, and LPs are not expected to provide as much timber as before.

Over the past 40 years, China has experienced rapid economic development and has become the second-largest economy in the world (Ouyang et al. 2016). Unfortunately, this process has been accompanied by a deteriorating environment. To continue the sustainable development and improve livelihoods and the environment, "ecological civilization" was presented as a national strategy in 2013. Since 2015, China has imposed total logging bans in natural forests to conserve natural forests and promote their non-timber ecosystem services. LPs are mainly distributed in mountain ranges, which are the sources or headwaters of the main rivers in Northeast China. These regions are of great importance to the water supply for agriculture and industry, as well as soil retention, biodiversity conservation, carbon sinks, recreational activities, etc. Here, the LP biomass estimate of 113 10^{12} g C accounts for approximately 5.6 % of the total forest biomass carbon storage in Northeast China (Guo et al. 2013). As an important part of the forest ecosystem, the regulating services of LPs should be recognized as vital to regional ecological security. Thus, multipurpose management practices should be carried out to inform policymakers and assure broader and sustainable benefits from LPs in the future.

The priorities of timber supply and regulating services (e.g., water conservation) of LPs should be reconsidered for planning multipurpose management strategies. The GSV represents the amount of current timber in a LP stand, which is closely related to its timber production (Gao et al. 2016) and can thus be applied as an important reference for multipurpose management plans. According to our estimates, the high GSV area (greater than 130 m^3 ha^{-1}) accounted for 9.0 % of the LP areas in Northeast China, and these areas mostly had good site conditions, as well as convenient traffic. These LPs can be managed as fast-growing and high-yielding plantations that can primarily meet the timber supply demands. The LPs with low GSV (less than 70 m^3 ha^{-1}) accounted for 28.5 % of the LP areas, and these areas had poor site conditions with steep slopes on mountains, which suppress timber production. The LP regulating services should be highlighted in these areas due to the high ecological vulnerability. Nonetheless, most of the LPs in China are planted as single species and even-aged stand structures that focus on timber production, which can threaten their regulating services (Rodriguez et al. 2006). Inducing LPs in the larch-broadleaved mixed forests (LBMF) has been recognized as an approach to improve the regulating services (Mason and Zhu 2014), and some studies have examined the feasibility of this method through thinning practices (Zhu et al. 2010; Gang, Yan, and Zhu 2015) and natural regeneration (Yan, Zhu, and Gang 2013). With the support of local LP management, these approaches can be applied to the LPs that are distributed in the mountain regions where environmental adjustment values clearly outweigh timber supply values. The rest of the area (70 m^3 ha^{-1} to 130 m^3 ha^{-1}) accounts for 62.5 % of the LP area where both timber production and regulating services would be taken into consideration. Trade-offs or synergies among multiple ecosystem services should be examined when quantifying ecosystem services in several forest management scenarios relative to potential forest management practices (e.g., inducing LBMF) to adjust the species composition of plantation forests. Research on the scenario trade-offs or synergies of a forest can pragmatically inform policy discussions and further support decisions related to plantation forest management planning (Zheng et al. 2016).

5. Conclusion

Using a combination of L-band SAR data and a ground-based inventory, an empirical model was developed to map LP GSV, and biomass was further estimated at a regional scale. The saturation effect of the ALOS PALSAR backscatter for the retrieval of LP GSV was examined at a high level, indicating its potential to be a reliable dataset for monitoring plantation forests. The GSV and biomass of LPs in Northeast China were estimated at 224 million m^3 and 113 10^{12} g C, respectively. Considering the current timber production and supply of China, as well as the growing environmental threats, the non-timber services of LPs should be highlighted. Based on the mapping result, this study tentatively proposed an explicit pattern for ecosystem service priority (which ecosystem services should be prioritized) that is simply linked to the LP GSV. To obtain broader and sustainable benefits from larch plantations, a more detailed multipurpose management plan should be created that systematically evaluates ecosystem services, as well as natural and social factors. In addition, as most forests provide a variety of services, including provision (e.g., timber production), support (e.g., soil formation), and regulation (e.g., water conservation), future studies should focus on the relationships (trade-offs and synergies) among ecosystem services when managing plantation forests in complex landscapes and regions.

Acknowledgements

This research was supported by the National Key Research and Development Program of China (2016YFD0600206), the National Natural Science Foundation of China (31500466) and the National Basic Research Program of China (973 Program, No. 2012CB416906). We thank members of sampling team of the Institute of Applied Ecology, Chinese Academy of Sciences (Yirong Sun, Guangqi Zhang, Chunyu Zhu, Liyan Huang, Guangchen Wang, Jingpu Zhang, Jing Wang, Ao Shen, Junxia Cong) for assistance with larch plantation field investigation. We would also be grateful to Shun Cheng of the Saihanba Forestry Center for sharing the Forest Resource Management Inventory data, and Hailong Sun of Northeast Forestry University, Ji Ye of Institute of Applied Ecology, Chinese Academy of Sciences for sharing allometric models of larch plantations.

Reference

Avtar, Ram, Rikie Suzuki, and Haruo Sawada. 2014. "Natural forest biomass estimation based on plantation information using PALSAR data." *PLoS ONE* 9 (1):e86121. doi: 10.1371/journal.pone.0086121.

Avtar, Ram, Wataru Takeuchi, and Haruo Sawada. 2013. "Monitoring of biophysical parameters of cashew plants in Cambodia using ALOS/PALSAR data." *Environ Monit Assess* 185 (2):2023-37.

Brown, Sandra L., Paul Schroeder, and Jeffrey S. Kern. 1999. "Spatial distribution of biomass in forests of the eastern USA." *Forest Ecology and Management* 123 (1):81-90.

Brown, Sandra, and E. Ariel Lugo. 1984. "Biomass of tropical forests: A new estimate based on forest volumes." *Science* 223 (4642):1290-3.

Carle, Jim, and Peter Holmgren. 2008. "Wood from Planted Forests A Global Outlook 2005-2030." *Forest Products Journal* 58 (12):6-18.

Cartus, Oliver, Maurizio Santoro, and Josef Kellndorfer. 2012. "Mapping forest aboveground biomass in the Northeastern United States with ALOS PALSAR dual-polarization L-band." *Remote Sensing of Environment* 124:466-78.

Chinese Ministry of Forestry. 2014. "Forest Resource Statistics of China." [In Chinese] Department of Forest Resource and Management, Chinese Ministry of Forestry, Beijing, China.

Chinese Ministry of Forestry. 2015. "Forestry development Report of China." [In Chinese] Department of Forest Resource and Management, Chinese Ministry of Forestry, Beijing, China.

Chave, J., C. Andalo, S. Brown, M. A. Cairns, J. Q. Chambers, D. Eamus, H. Fölster, et al. 2005. "Tree allometry and improved estimation of carbon stocks and balance in tropical forests." *Oecologia* 145 (1):87-99. doi: 10.1007/s00442-005-0100-x.

Chave, Jerome, Richard Condit, Salomon Aguilar, Andres Hernandez, Suzanne Lao, and Rolando Perez. 2004. "Error propagation and scaling for tropical forest biomass estimates." *Philosophical Transactions of the Royal Society B: Biological Sciences* 359 (1443):409-20.

Chowdhury, Tanvir Ahmed, Christian Thiel, and Christiane Schmullius. 2014. "Growing stock volume estimation from L-band ALOS PALSAR polarimetric coherence in Siberian forest." *Remote Sensing of Environment* 155:129-44.

Costanza, Robert, Ralph D'Arge, Rudolf de Groot, Stephen Farber, Monica Grasso, Bruce Hannon, Karin Limburg, et al. 1997. "The value of the world's ecosystem services and natural capital." *Nature* 387 (6630):253-60.

Cutler, M. E. J., D. S. Boyd, G. M. Foody, and A. Vetrivel. 2012. "Estimating tropical forest biomass with a combination of SAR image texture and Landsat TM data: An assessment of predictions between regions." *ISPRS Journal of Photogrammetry and Remote Sensing* 70:66-77.

Department of Forestry of Inner Mongolia Autonomous Region. 1993. “Tree Volume Table of Department of Forestry of Inner Mongolia Autonomous Region.” [In Chinese] Department of Forestry of Inner Mongolia Autonomous Region, Hohhot, China.

Department of Forestry of Liaoning Province. 1994. “Tree Volume Table of Liaoning province.” [In Chinese] Department of Forestry of Liaoning Province. Shenyang, China.

Department of Forestry of Heilongjiang Province. 1998. “Tree Volume Table of

Heilongjiang province.” [In Chinese] Department of Forestry of Heilongjiang Province. Harbin, China.

Department of Forestry of Jilin Province. 2002. “Tree Volume Table of Jilin province.” [In Chinese] Department of Forestry of Jilin Province. Changchun, China.

Fang, Jingyun, Anping Chen, Changhui Peng, Shuqing Zhao, and Longjun Ci. 2001. "Changes in forest biomass carbon storage in China between 1949 and 1998." *Science* 292 (5525):2320-2.

Fang, Jingyun, G. Geoff Wang, Guohua Liu, and Songling Xu. 1998. "Forest biomass of China: An estimate based on the biomass–volume relationship." *Ecological Applications* 8 (4):1084-91.

Fang, Jingyun, and Zhangming Wang. 2001. "Forest biomass estimation at regional and global levels, with special reference to China's forest biomass." *Ecological Research* 16 (3):587-92.

Food and Agriculture Organization, 2010. “Food and Agriculture Organization Resources Assessment 2010.” In, Rome, pp. 90.

Gang, Qun, Qiaoling Yan, and JiaoJun Zhu. 2015. "Effects of thinning on early seed regeneration of two broadleaved tree species in larch plantations: implication for converting pure larch plantations into larch-broadleaved mixed forests." *Forestry* 88 (5):573-85.

Gao, Tian, Jiaojun Zhu, Songqiu Deng, Xiao Zheng, Jinxin Zhang, Guiduo Shang, and Liyan Huang. 2016. "Timber production assessment of a plantation forest: An integrated framework with field-based inventory, multi-source remote sensing data and forest management history." *International Journal of Applied Earth Observation and Geoinformation* 52:155-65.

Gao, Tian, Jiaojun Zhu, Xiao Zheng, Guiduo Shang, Liyan Huang, and Shangrong Wu. 2015. "Mapping spatial distribution of larch plantations from multi-seasonal Landsat-8 OLI imagery and multi-scale textures using random forests." *Remote Sensing* 7 (2):1702-20. doi: 10.3390/rs70201702.

Gu, C. 1985. "A Study on the Increment of Main Forest Communities in the Forest Region of the Daxingan Mountain." [In Chinese] Journal of North-east Forestry University 15, 108-114.

Guo, Zhaodi, Jingyun Fang, Yude Pan, and Richard Birdsey. 2010. "Inventory-based estimates of forest biomass carbon stocks in China: A comparison of three methods." *Forest Ecology and Management* 259 (7):1225-31.

Guo, Zhaodi, Huifeng Hu, Pin Li, Nuyun Li, and Jingyun Fang. 2013. "Spatio-temporal changes in biomass carbon sinks in China's forests from 1977 to 2008." *Science China Life Sciences* 56 (7):661-71.

Hamdan, O., H. Khali Aziz, and I. Mohd Hasmadi. 2014. "L-band ALOS PALSAR for biomass estimation of Matang Mangroves, Malaysia." *Remote Sensing of Environment* 155 (0):69-78.

Imhoff, M. L. 1995. "Radar backscatter and biomass saturation: ramifications for global biomass inventory." *Geoscience and Remote Sensing, IEEE Transactions on* 33 (2):511-8.

Immitzer, Markus, Christoph Stepper, Sebastian Böck, Christoph Straub, and Clement

Atzberger. 2016. "Use of WorldView-2 stereo imagery and National Forest Inventory data for wall-to-wall mapping of growing stock." *Forest Ecology and Management* 359:232-46.

Isaev, A., G. Korovin, D. Zamolodchikov, A. Utkin, and A. Pryaznikov. 1995. “Carbon Stock and Deposition in Phytomass of the Russian Forests.” Water, Air, and Soil Pollution 82 (1): 247-256.

Kanninen, M. 2010. "Plantation forests: global perspectives." In *Ecosystem goods and services from plantation forests*, edited by J. Bauhus, P. van der Meer and M. Kanninen, 1-15. London: Earthscan.

Karam, Mostafa A., Faouzi Amar, Adrian K. Fung, Eric Mougin, Armand Lopes, David M. Le Vine, and André Beaudoin. 1995. "A microwave polarimetric scattering model for forest canopies based on vector radiative transfer theory." *Remote Sensing of Environment* 53 (1):16-30.

Kira, T. 1976. "Terrestrial Ecosystem: A General Introduction. " Kyoritus-shuppan, Tokyo, Japan.

Lee, J. S., J. H. Wen, T. Ainsworth, K. S. Chen, and A. Chen. 2009. "Improved sigma filter for speckle filtering of SAR imagery." *IEEE Transactions on Geoscience and Remote Sensing* 47:202-13.

Lucas, R. M., J. Armston, R. Fairfax, R. Fensham, A. Accad, J. Carreiras, and More Authors. 2010. "An evaluation of the ALOS PALSAR L-band backscatter-above ground biomass relationship Queensland, Australia: impacts of surface moisture condition and vegetation structure." *IEEE Journal of*

Selected Topics in Applied Earth Observations and Remote Sensing 4 (3):576-93.

Mason, W. L., and J. J. Zhu. 2014. "Silviculture of Planted Forests Managed for Multi-functional Objectives: Lessons from Chinese and British Experiences." In *Challenges and Opportunities for the World's Forests in the 21st Century*, edited by Trevor Fenning, 37-54. Dordrecht: Springer Netherlands.

Meng, X. 2005. "Forest Measuration (the 2nd edition)". [In Chinese] China Forestry Publishing House, Beijing.

Mermoz, Stéphane, Thuy Le Toan, Ludovic Villard, Maxime Réjou-Méchain, and Joerg Seifert-Granzin. 2014. "Biomass assessment in the Cameroon savanna using ALOS PALSAR data." *Remote Sensing of Environment* 155 (0):109-19.

Mitchard, E. T. A., S. S. Saatchi, I. H. Woodhouse, G. Nangendo, N. S. Ribeiro, M. Williams, C. M. Ryan, S. L. Lewis, T. R. Feldpausch, and P. Meir. 2009. "Using satellite radar backscatter to predict above-ground woody biomass: A consistent relationship across four different African landscapes." *Geophysical Research Letters* 36 (23):L23401.

Morel, Alexandra C., Joshua B. Fisher, and Yadvinder Malhi. 2012. "Evaluating the potential to monitor aboveground biomass in forest and oil palm in Sabah, Malaysia, for 2000–2008 with Landsat ETM+ and ALOS-PALSAR." *International Journal of Remote Sensing* 33 (11):3614-3639. doi: 10.1080/01431161.2011.631949 doi: 10.1080/01431161.2011.631949.

Mougin, E., C. Proisy, G. Marty, F. Fromard, H. Puig, J. L. Betoulle, and J. P. Rudant. 1999. "Multifrequency and multipolarization radar backscattering from mangrove forests." *IEEE Transactions on Geoscience and Remote Sensing* 37 (1):94-102.

Ouyang, Zhiyun, Hua Zheng, Yi Xiao, Stephen Polasky, Jianguo Liu, Weihua Xu, Qiao Wang, et al. 2016. "Improvements in ecosystem services from investments in natural capital." *Science* 352 (6292):1455.

Pan, Yude, Richard A. Birdsey, Jingyun Fang, Richard Houghton, Pekka E. Kauppi, Werner A. Kurz, Oliver L. Phillips, et al. 2011. "A large and persistent carbon sink in the world's forests." *Science* 333:988-93.

Pantze, Andreas, Maurizio Santoro, and Johan E. S. Fransson. 2014. "Change detection of boreal forest using bi-temporal ALOS PALSAR backscatter data." *Remote Sensing of Environment* 155:120-8.

Pen, Kefeng. 2015. “Article Title.” China Science Daily, October 26.

Peregon, Anna, and Yoshiki Yamagata. 2013. "The use of ALOS/PALSAR backscatter to estimate above-ground forest biomass: A case study in Western Siberia." *Remote Sensing of Environment* 137 (0):139-46.

Rahman, M. Mahmudur, and Josaphat Tetuko Sri Sumantyo. 2012. "Retrieval of tropical forest biomass information from ALOS PALSAR data." *Geocarto International* 28 (5):382-403. doi: 10.1080/10106049.2012.710652 2014/10/17 doi: 10.1080/10106049.2012.710652.

Robinson, Chelsea, Sassan Saatchi, Maxim Neumann, and Thomas Gillespie. 2013.

"Impacts of spatial variability on aboveground biomass estimation from l-band radar in a temperate forest." *Remote Sensing* 5:1001-23. doi: 10.3390/rs5031001.

Rodriguez-Galiano, V. F., M. Chica-Olmo, F. Abarca-Hernandez, P. M. Atkinson, and C. Jeganathan. 2012. "Random Forest classification of Mediterranean land cover using multi-seasonal imagery and multi-seasonal texture." *Remote Sensing of Environment* 121:93-107.

Rodriguez, Jon Paul, T. Douglas Beard, Elena M. Bennett, Graeme S. Cumming, Steven J. Cork, John Agard, Andrew P. Dobson, and Garry D. Peterson. 2006. "Trade-Offs Across Space, Time, and Ecosystem Services." *Ecology and Society* 11.

Rosenqvist, A., M. Shimada, N. Ito, and M. Watanabe. 2007. "ALOS PALSAR: A pathfinder mission for global-scale monitoring of the environment." *Geoscience and Remote Sensing, IEEE Transactions on* 45 (11):3307-16.

Saatchi, Sassan, Miriam Marlier, Robin L. Chazdon, David B. Clark, and Ann E. Russell. 2011. "Impact of spatial variability of tropical forest structure on radar estimation of aboveground biomass." *Remote Sensing of Environment* 115 (11):2836-49.

Saatchi, Sassan, and Mahta Moghaddam. 2000. "Estimation of crown and stem water content and biomass of boreal forest using polarimetric SAR imagery." *IEEE Transactions on Geoscience and Remote Sensing* 38 (2):697-709.

Saihanba Forestry Center, 2012. “Forest Resource Plan and Inventory Report (4^{th}) of

Saihanba Forestry Center of Hebei Province.” [In Chinese] Saihanba Forestry Center, Hebei, China.

Sandberg, G., L. M. H. Ulander, J. E. S. Fransson, J. Holmgren, and T. Le Toan. 2011. "L- and P-band backscatter intensity for biomass retrieval in hemiboreal forest." *Remote Sensing of Environment* 115 (11):2874-86.

Santoro, Maurizio, Leif Eriksson, and Johan Fransson. 2015. "Reviewing ALOS PALSAR backscatter observations for stem volume retrieval in Swedish forest." *Remote Sensing* 7 (4):4290-317. doi: 10.3390/rs70404290.

Sarker, Md Latifur Rahman, Janet Nichol, Baharin Ahmad, Ibrahim Busu, and Alias Abdul Rahman. 2012. "Potential of texture measurements of two-date dual polarization PALSAR data for the improvement of forest biomass estimation." *ISPRS Journal of Photogrammetry and Remote Sensing* 69:146-66.

Schlund, Michael, Felicitas von Poncet, Steffen Kuntz, Christiane Schmullius, and Dirk H. Hoekman. 2015. "TanDEM-X data for aboveground biomass retrieval in a tropical peat swamp forest." *Remote Sensing of Environment* 158 (0):255-66.

Schroeder, Paul, Sandra Brown, Jiangming Mo, Richard Birdsey, and Chris Cieszewski. 1997. "Biomass estimation for temperate broadleaf forests of the United States using inventory data." *Forest Science* 43 (3):424-34.

Shang, Guiduo, Zhu Jiaojun, Gao Tian, Zheng Xiao, Zhang Jinxin. 2017. "Using multi-source remote sensing data to classify larch plantations in Northeast China and support the development of multi-purpose silviculture." *Journal* *of Forestry Research* doi: 10.1007/s11676-017-0518-0.

Sharp, Douglas D., Helmut Lieth, and Dennis Whigham. 1975. "Assessment of Regional Productivity in North Carolina." In *Primary Productivity of the Biosphere*, edited by Helmut Lieth and Robert H. Whittaker, 131-46. Berlin, Heidelberg: Springer Berlin Heidelberg.

Shimada, M., O. Isoguchi, T. Tadono, and K. Isono. 2009. "PALSAR Radiometric and Geometric Calibration." *IEEE Transactions on Geoscience and Remote Sensing* 47 (12):3915-32.

Shimada, M., and T. Ohtaki. 2010. "Generating large-scale high-quality SAR mosaic datasets: Application to PALSAR data for global monitoring." *IEEE Journal of Selected Topics in Applied Earth Observations and Remote Sensing* 3 (4):637-56.

Shimada, Masanobu, Takuya Itoh, Takeshi Motooka, Manabu Watanabe, Tomohiro Shiraishi, Rajesh Thapa, and Richard Lucas. 2014. "New global forest/non-forest maps from ALOS PALSAR data (2007-2010)." *Remote Sensing of Environment* 15:13-31.

Slayback, D. J., S. Los Pinzon, and C. J. Tucker. 2003. "Northern hemisphere photosynthetic trends 1982-99." *Global Change Biology* 9 (1):1-15.

Thiel, Christian, and Christiane Schmullius. 2016. "The potential of ALOS PALSAR backscatter and InSAR coherence for forest growing stock volume estimation in Central Siberia." *Remote Sensing of Environment* 173:258-73.

Turner, David P., Greg J. Koerper, Mark E. Harmon, and Jeffrey J. Lee. 1995. "A carbon budget for forests of the conterminous United States." *Ecological Applications* 5 (2):421-36.

UNDP (United Nations Development Program), and IUES (Institute for Urban and Environmental Studies). 2013. "China National Human Development Report 2013 Sustainable and Liveable Cities: Toward Ecological Civilization". China Publishing Group Corporation, Beijing.

Wang, Xiangping, Jingyun Fang, and Biao Zhu. 2008. "Forest biomass and root-shoot allocation in northeast China." *Forest Ecology and Management* 255 (12):4007-20.

Watanabe, M., M. Shimada, A. Rosenqvist, T. Tadono, M. Matsuoka, Shakil Ahmad Romshoo, K. Ohta, R. Furuta, K. Nakamura, and T. Moriyama. 2006. "Forest structure dependency of the relation between L-Band sigma and biophysical parameters." *Geoscience and Remote Sensing, IEEE Transactions on* 44 (11):3154-65.

Wilhelm, Sebastian, Christian Hüttich, Mikhail Korets, and Christiane Schmullius. 2014. "Large area mapping of boreal growing stock volume on an annual and multi-temporal level using PALSAR L-band backscatter mosaics." *Forests* 5 (8):1999-2015. doi: 10.3390/f5081999.

Yan, Qiaoling, Jiaojun Zhu, and Qun Gang. 2013. "Comparison of spatial patterns of soil seed banks between larch plantations and adjacent secondary forests in Northeast China: implication for spatial distribution of larch plantations." *Trees* 27 (6):1747-54.

Yang, Kai, Jiaojun Zhu, Qiaoling Yan, and Jinxin Zhang. 2012. "Soil enzyme activities as potential indicators of soluble organic nitrogen pools in forest ecosystems of Northeast China." *Annals of Forest Science* 69 (7):795-803.

Yang, Kai, Jiaojun Zhu, Min Zhang, Qiaoling Yan, and Osbert Jianxin Sun. 2010. "Soil microbial biomass carbon and nitrogen in forest ecosystems of Northeast China: a comparison between natural secondary forest and larch plantation." *Journal of Plant Ecology* 3 (3):175 -82.

Zheng, Hua, Yifeng Li, Brian E. Robinson, Gang Liu, Dongchun Ma, Fengchun Wang, Fei Lu, Zhiyun Ouyang, and Gretchen C. Daily. 2016. "Using ecosystem service trade-offs to inform water conservation policies and management practices." *Frontiers in Ecology and the Environment* 14 (10):527-32.

Zhu, J. J., Z. G. Liu, H. X. Wang, Q. L. Yan, H. Y. Fang, L. L. Hu, and L. Z. Yu. 2008. "Effects of site preparation on emergence and early establishment of Larix olgensis in montane regions of northeastern China." *New Forests* 36 (3):247-60.

Zhu, Jiaojun, Kai Yang, Qiaoling Yan, Zugen Liu, Lizhong Yu, and Hexin Wang. 2010. "Feasibility of implementing thinning in even-aged Larix olgensis plantations to develop uneven-aged larch-broadleaved mixed forests." *Journal of Forest Research* 15 (1):71-80.

Table 1 Allometric models for volume calculation of larch plantation. The allometric models were collected from the forestry administrations (Department of Forestry of Inner Mongolia Autonomous Region 1993; Department of Forestry of Liaoning Province 1994; Department of Forestry of Heilongjiang Province 1998; Department of Forestry of Jinlin Province 2002; Saihanba Forestry Center 2012). *V* (m^3) is the stand stem volume of trees and *D* (cm) is the diameter at breast height of trees.

Table 2 Growing stock volume (*y*) estimation accuracy of regression models expressed in terms of R^2 (the coefficient of determination), RMSE and rRMSE for five independent variables (*x*) from ALOS PALSAR polarisations. *The model samples and test samples were 276 and 104, respectively. The model accuracy tested by the samples that GSV is less than 245 m^3 ha^{-1}.

Table 3 Comparison of saturation levels of L-band SAR data for GSV estimation among different studies. Only GSV was documented in the original references. To compare saturation levels among different studies, saturation level expressed by GSV (m^3 ha^{-1}) were convert to AGB (10^6 g ha^{-1}). A mean BEF (0.88) for the Russian taiga forests (Isaev et al. 1995) and mean ratios (0.71) of AGB to total biomass (Kira 1976) were applied to estimate the saturation levels of AGB (10^6 g ha^{-1}). The ratios (0.83) of AGB to total biomass of LP were used to convert total biomass to AGB (Wang et al. 2008).

Figure 1 Locations of the sampling sites across Northeast China. Some plots overlap visually each other and are therefore invisible. The numbers of samples are 64 for 2011, 36 for 2013, 166 for 2014 and 114 for 2015, respectively.

Figure 2 Relationships between the variables of ALOS PALSAR polarisations and growing stock volume (GSV). The ground truth GSV samples were plotted against variables, including HH (*a*), HV (*b*), HV / HH (*c*), (HV + HH) / 2 (*d*) and $(HH \cdot HV)^{-1/2}$ (*e*). Scatterplots of ground truth GSV against the retrieved GSV by the best variable ((HV + HH) / 2) (*f*).

Figure 3 Spatial distribution of LP GSV.

Figure 4 Spatial distribution of LP BEF (*a*) and biomass (*b*).

Table 1 Allometric models for volume calculation of larch plantation. The allometric models were collected from the forestry administrations (Department of Forestry of Inner Mongolia Autonomous Region 1993; Department of Forestry of Liaoning Province 1994; Department of Forestry of Heilongjiang Province 1998; Department of Forestry of Jinlin Province 2002; Saihanba Forestry Center 2012). V (m^3) is the stand stem volume of trees and D (cm) is the diameter at breast height of trees.

Region	Allometric model
Northern Hebei Province	$V = 0.000095\ D^{2.561805}$
Liaoning Province	$V = 0.000083\ D^{2.626108}$
Jilin Province	$V = 0.000208\ D^{2.371992}$
Heilongjiang Province	$V = 0.000126\ D^{2.483454}$
Inner Mongolia Autonomous Region	$V = 0.000069\ D^{2.685323}$

Table 2 Growing stock volume (y) estimation accuracy of regression models expressed in terms of R^2 (the coefficient of determination), RMSE and rRMSE for five independent variables (x) from ALOS PALSAR polarisations. *The model samples and test samples were 276 and 104, respectively. The model accuracy tested by the samples that GSV is less than 245 $m^3\ ha^{-1}$.

Variable	Model	R^2	RMSE ($m^3\ ha^{-1}$)	rRMSE (%)	RMSE* ($m^3\ ha^{-1}$)	rRMSE* (%)
HH	$y = 1.9621 \ln(x) - 15.603$	0.549	± 46.565	36.957	± 41.840	33.206
HV	$y = 2.8387 \ln(x) - 25.255$	0.637	± 39.125	31.051	± 34.668	27.514
HV / HH	$y = 0.0962 \ln(x) + 1.475$	0.057	± 121.709	96.594	± 112.674	89.424
(HH + HV) / 2	$y = 2.4004 \ln(x) - 20.429$	0.638	± 37.546	29.799	± 33.104	26.273
$(HH \cdot HV)^{-1/2}$	$y = -2.3710 \ln(x) + 19.835$	0.623	± 40.148	31.864	± 35.669	28.309

Table 3 Comparison of saturation levels of L-band SAR data for GSV estimation among different studies. Only GSV was documented in the original references. To compare saturation levels among different studies, saturation level expressed by GSV (m^3 ha^{-1}) were convert to AGB (10^6 g ha^{-1}). A mean BEF (0.88) for the Russian taiga forests (Isaev et al. 1995) and mean ratios (0.71) of AGB to total biomass (Kira 1976) were applied to estimate the saturation levels of AGB (10^6 g ha^{-1}). The ratios (0.83) of AGB to total biomass of LP were used to convert total biomass to AGB (Wang et al. 2008).

Forest type	Study Site	Saturation level (10^6 g ha^{-1})	Reference
Cashew plantation	Cambodia	100	(Avtar, Suzuki, and Sawada. 2014)
Mangrove	Malaysia	125	(Hamdan, Khali Aziz, and Mohd Hasmadi 2014)
Tropics forest	Costa Rica	100	(Saatchi et al. 2011)
Savanna	Cameroon	100	(Mermoz et al. 2014)
Temperate forest	Northeastern United States	200	(Cartus, Santoro, and Kellndorfer 2012)
Boreal forest	Central Siberia	145 (230 m^3 ha^{-1})	(Thiel and Schmullius 2016)
Boreal forest	Siberia	157 (250 m^3 ha^{-1})	(Chowdhury et al. 2014)
Larch plantation	Northeast China	160 (260 m^3 ha^{-1})	This study

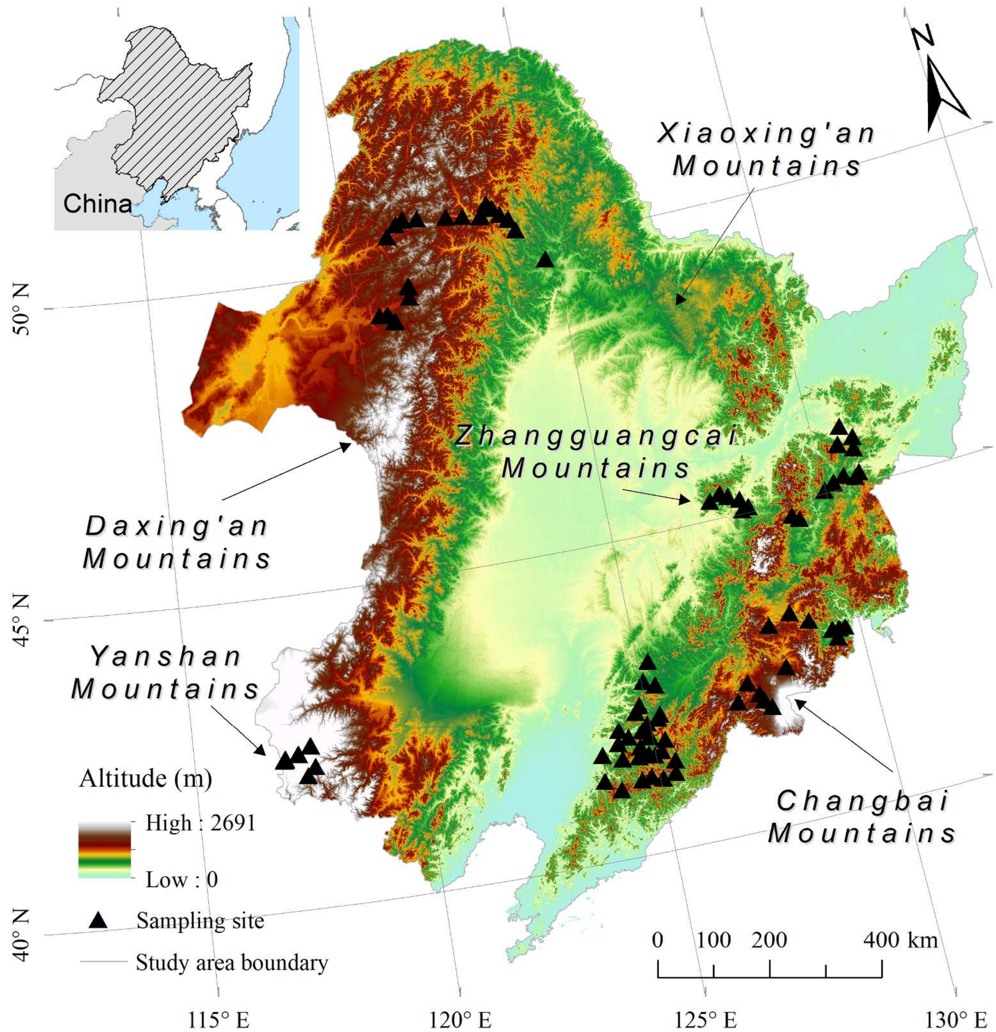

Figure 1 Locations of the sampling sites across Northeast China. Some plots overlap visually each other and are therefore invisible. The numbers of samples are 64 for 2011, 36 for 2013, 166 for 2014 and 114 for 2015, respectively.

210x219mm (300 x 300 DPI)

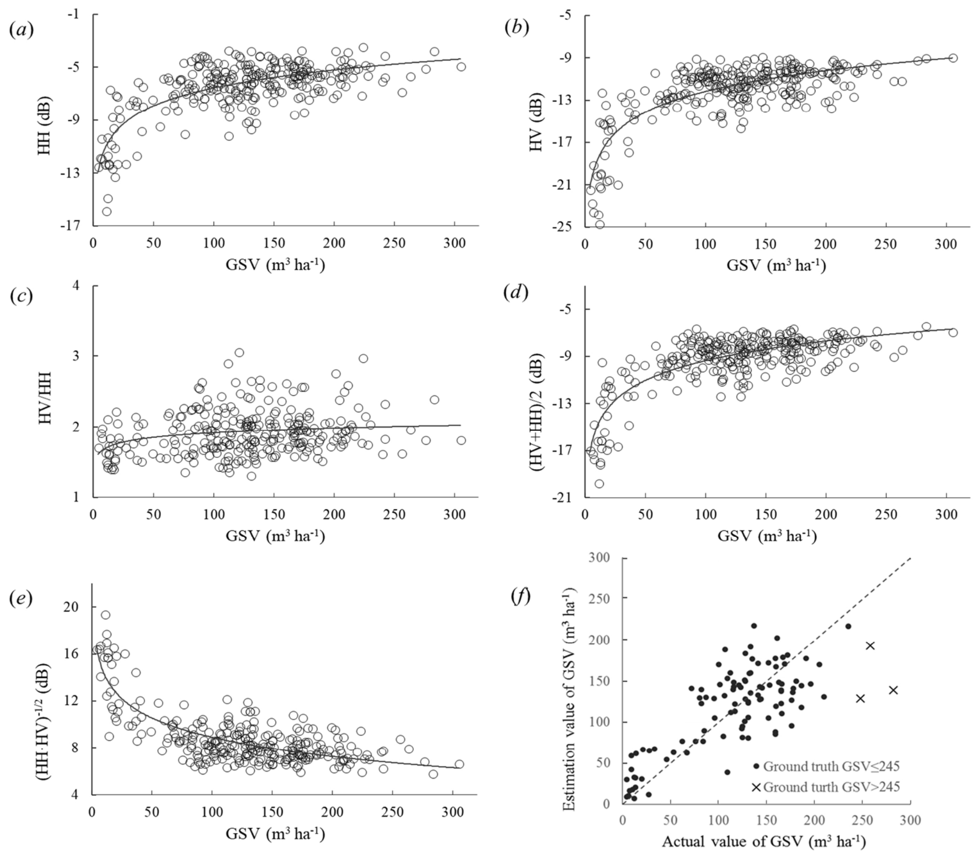

Figure 2 Relationships between the variables of ALOS PALSAR polarisations and growing stock volume (GSV). The ground truth GSV samples were plotted against variables, including HH (*a*), HV (*b*), HV / HH (*c*), (HV + HH) / 2 (*d*) and $(HH \cdot HV)^{-1/2}$ (*e*). Scatterplots of ground truth GSV against the retrieved GSV by the best variable ((HV + HH) / 2) (*f*).

750x636mm (96 x 96 DPI)

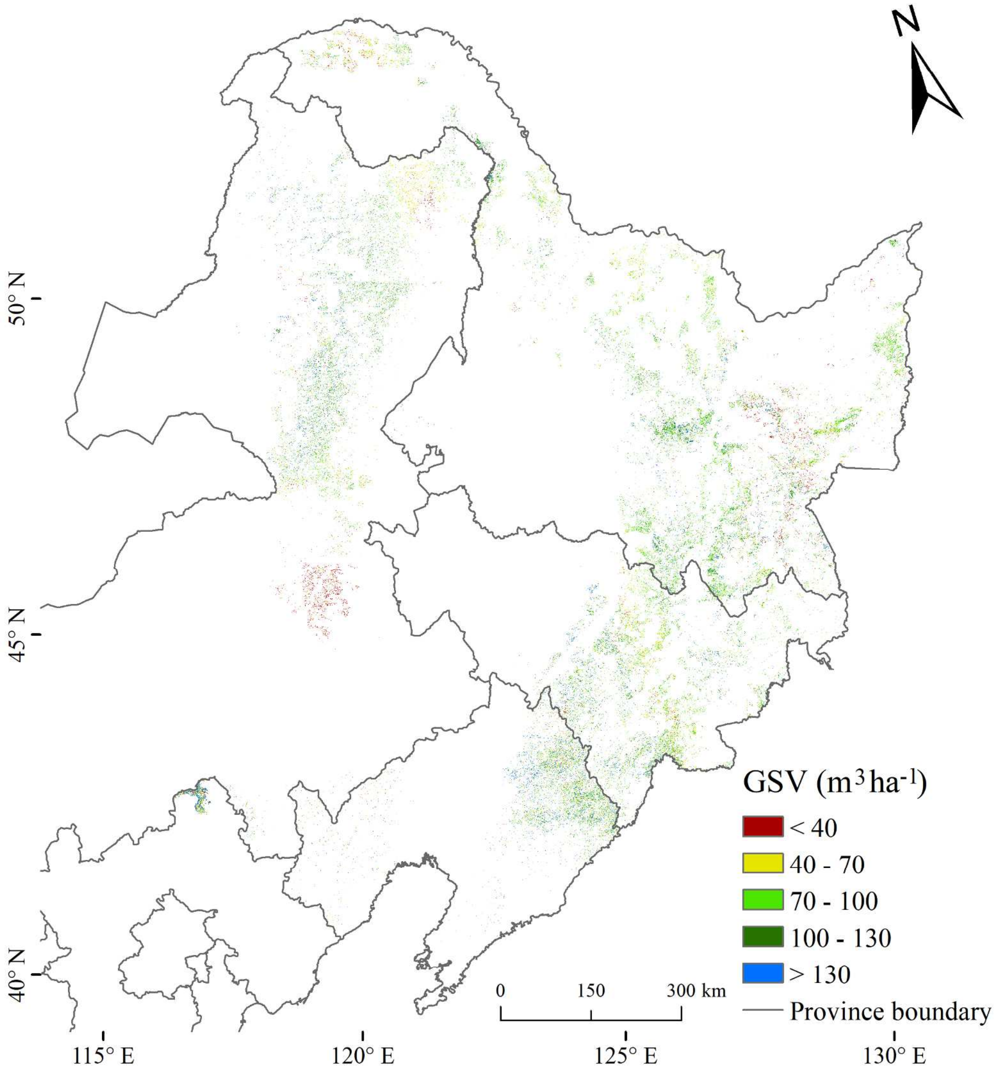

Figure 3 Spatial distribution of LP GSV.

210x229mm (300 x 300 DPI)

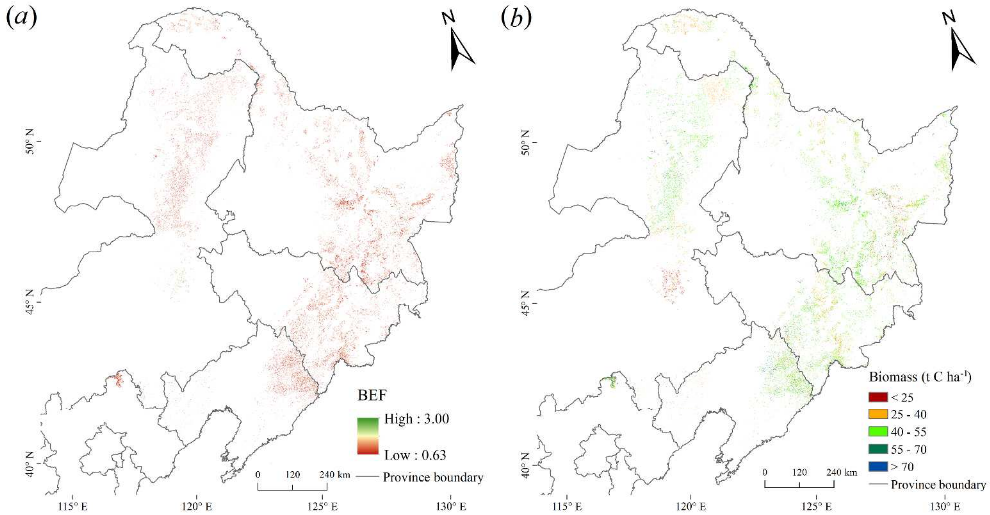

Figure 4 Spatial distribution of LP BEF (*a*) and biomass (*b*).

440x229mm (300 x 300 DPI)